NASA Contractor Report 198388

Conceptual Design of a Vapor Core Reactor Rocket Engine for Space Propulsion

E.T. Dugan, N.J. Diaz, S.A. Kuras,
S.P. Keshavmurthy, and I. Maya
University of Florida
Gainesville, Florida

April 1996

Prepared for
Lewis Research Center
Under Contract NAS3–26314

National Aeronautics and
Space Administration

Conceptual Design of a Vapor Core Reactor Rocket Engine for Space Propulsion

ABSTRACT

Neutronic, thermal hydraulic, and thermal mechanical studies have been performed on an innovative vapor core nuclear reactor concept for space propulsion. The Nuclear Vapor Thermal Reactor (NVTR) Rocket Engine uses modified-NERVA geometry and systems with the solid fuel replaced by uranium tetrafluoride vapor.

The use of C-C composite fuel elements in the NVTR leads to a compact reactor with low critical mass, good power peaking characteristics, an overall negative power coefficient of reactivity and, hence, good stability, and a propulsion system with high specific impulse. Thermo-mechanical analysis has shown excellent thermo-mechanical behavior under the high power density, high temperature NVTR environment.

The NVTR is an intermediate term gas core thermal rocket engine with specific impulse in the range of 1000-1200 seconds; a thrust of 75,000 lbs. for a hydrogen flow rate of 30 kg/s; average core exit temperatures of 3100 K to 3400 K; reactor thermal powers of 1400 to 1800 MW; and thrust-to-weight ratios of 5-to-1.

TABLE OF CONTENTS

TABLES

FIGURES

(Figures Located at end of Report)

1.0 INTRODUCTION

Solid core reactors provide the path for minimum risk for generating nuclear space power in the near-term. These reactors can be expected to achieve evolutionary improvements in their performance based on modest extrapolations of current fuel technology. In contrast, Gas Core Reactors (GCRs) offer a longer path with extraordinary improvements in performance, and have the highest potential for reducing overall system specific mass. The nearest term technology for development of GCRs, offering modest gains over solid core reactors, is the Nuclear Vapor Thermal Reactor (NVTR).

The NVTR core, shown in Figure 1 in a rocket engine, uses modified-NERVA geometry and systems with the solid fuel replaced by highly enriched (>85%) uranium tetrafluoride (UF_4) vapor; the cell geometry is changed to achieve neutronic and heat transfer requirements. The NVTR employs a graphite-moderated reactor and hydrogen propellant to regeneratively cool the structure and moderator. Studies have been performed both on epithermal NVTRs using ZrC fuel elements and thermal NVTRs using C-C composite fuel elements. The NVTR has a heterogeneous core which typically contains a lattice of thousands

term gas core thermal rocket engine. In the NVTR, the hydrogen propellant is the primary coolant and is physically separated from the non-circulating UF_4 fuel gas. This represents a major departure from previous HGCR designs and consequently, the NVTR unit cell and core design require a completely new set of neutronic, thermal, and materials analyses and optimization studies.

2.0 NEUTRONIC ANALYSIS METHODOLOGY

For the NVTR multigroup and few group neutronic calculations, the AMPX system[5] 1D, S_n transport theory XSDRNPM code was used for generating group constants. 123 group (30 thermal group) unit cell calculations were performed in cylindrical geometry with XSDRNPM on the NVTR fuel element to generate collapsed group cross sections. The XSDRNPM unit cell calculations also provided core k_∞ values. However, because of the large neutron mean free path in the UF_4 fuel gas region, perpendicular leakage effects cannot be accounted for by means of conventional buckling type corrections and the 1D XSDRNPM k_∞ values are found to be in significant error (-10% $\Delta k/k$) when compared with results from DOT-4[6], 2D S_n transport theory and MCNP[7] 3D, Monte Carlo calculations. Typical atom densities used in the NVTR analysis are found in Table 1.

Neutron multiplication factor (k_{eff}) calculations were performed on the NVTR using XSDRNPM, DOT4, and MCNP in one, two, and three dimensions, respectively. The XSDRNPM and DOT4 k_{eff} calculations employed the collapsed or homogenized group constants from the XSDRNPM unit cell runs. The MCNP calculations used a continuous energy analysis on the actual geometry. Because of the above mentioned difficulty in treating perpendicular leakage effects, the 1D XSDRNPM reactor calculations were performed on an "equivalent" spherical configuration with the same volume core and same thickness reflector as the actual cylindrical system. For nearly "square" cylinders (core diameter $\simeq$ core height or aspect ratio near unity), the XSDRNPM k_{eff} is in error by only about 1% to 2% as compared to 2D DOT4 results. For aspect ratios less than 0.5 or greater than 2.0, the error in the k_{eff} value from the "equivalent" sphere approximation becomes significant and is not used.

NVTRs using ZrC fuel elements are epithermal reactors with only 40 to 60% of the fissions occurring in the thermal energy range (see Table 2). For a given core size and reflector thickness, the k_{eff} depends on both the selected unit fuel cell dimensions and the UF_4 pressure. However, for this epithermal NVTR it has been found that the k_{eff} variation can essentially be reduced to a dependence on a single quantity, the fuel-to-moderator (F/M) atom ratio. Thus, different combinations of cell dimensions and UF_4 pressures that yield the same F/M ratio yield essentially the same k_{eff} and k_{eff} is found to continuously increase with increasing F/M ratio. As a consequence, optimized cell dimensions are dictated largely by thermal mechanical and thermal hydraulic rather than by neutronic considerations.

NVTRs using C-C composite fuel elements are thermal reactors in which typically 85% or more of the fissions occur in the thermal energy range (see Table 2). Unlike for the ZrC systems, neutronic optimization of the unit fuel cell is an important consideration when selecting overall, optimized cell dimensions. Because of the additional degree of freedom

associated with the vapor fuel density, unit cell neutronic optimization for this reactor is more complex than for conventional solid fuel, thermal reactors. To start the unit cell neutronic optimization process, a convenient fuel element flat-to-flat distance (FFD) or "equivalent" cylindrical cell outer radius is chosen for a fixed fuel radius, r_f. The UF_4 pressure is varied and k_{eff} is plotted versus UF_4 pressure. Following a steady increase in k_{eff} with pressure, the curve "saturates" and increases in UF_4 pressure beyond the saturation point yield diminishingly small gains in k_{eff}.

After selecting a pressure that is usually somewhat below the saturation point, r_f is fixed and FFD is varied. A plot of k_{eff} versus FFD, or versus the corresponding (F/M) atom ratio, shows a peak value of k_{eff} for some F/M value. An F/M value is then selected that is near the optimum, but representative of a slightly overmoderated system. For this fixed F/M, r_f is then varied and k_{eff} is plotted versus the fuel region radius. This curve also exhibits a peak, but selection of the final cell dimensions must include manufacturing, thermal hydraulic, and thermal mechanical, as well as neutronic considerations.

3.0 NEUTRONIC ANALYSIS RESULTS

Analysis of the ZrC-moderated NVTR led to the selection of a unit fuel cell that has a central UF_4 vapor channel radius of 1.1 cm, 32 hydrogen coolant/propellant channels each with a diameter of 0.14 cm, and an FFD for the hexagonal element of 3.3 cm (see Figure 1). Volume fractions for UF_4 vapor fuel, ZrC moderator, and hydrogen propellant in the fuel element are 0.40, 0.55 and 0.05, respectively. The UF_4 and hydrogen are both at a pressure of 10^7 pascals (~ 100 atmospheres) and have core average temperatures of ~4500 K and ~1700 K, respectively. This yields an F/M ratio of $4x10^{-3}$. Figure 2 shows k_{eff} versus F/M ratio for the ZrC-moderated NVTR.

A 75 klb_f thrust NVTR core based on ZrC moderation contains almost 4000 fuel elements and has a radius of 120 cm and a height of 150 cm. The large size of this core is dictated by thermal rather than neutronic considerations. The ZrC heat flux limit of 333 W/cm^2 requires a large surface area and, hence, a large core to achieve the approximately 1800 MW needed for a 75 klb thrust NVTR. By coincidence, this particular core size corresponds to a value where k_{eff} essentially begins to saturate (see Figure 3). That is, for the given fuel element configuration and UF_4 pressure, further increases in core size yield very small increases in k_{eff}. Criticality can easily be achieved with much smaller cores; for example, with R=60 cm and H=120 cm and a core volume that is about five times smaller. However, the ZrC heat flux limit restricts the power in such a core to around 360 MW.

Neutronic analysis has shown that comparatively little increase in neutron multiplication factor (k_{eff}) occurs for BeO reflector thicknesses beyond 30 to 40 cm (see Figure 4). For the ZrC-moderated NVTR both the radial BeO reflector and top axial BeO reflector have a thickness of 30 cm; the bottom axial reflector is a 30 cm thick C-C composite.

Reactivity coefficients have been obtained for the ZrC NVTR. The fuel temperature coefficient is very small and negative with a value of $-2x10^{-7}$ $\Delta k/k$ per K. The hydrogen

pressure coefficient is of moderate size and positive with a value of 4.5×10^{-4} $\Delta k/k$ per atmosphere. The graphite moderator temperature coefficient of reactivity is small and positive with a value of 2.0×10^{-6} $\Delta k/k$ per K while the BeO reflector temperature coefficient of reactivity is moderate and positive with a value of 2×10^{-5} $\Delta k/k$ per K. Finally, the hydrogen coolant temperature coefficient of reactivity is small and positive with a value of 2×10^{-7} $\Delta k/k$ per K. (Typical coefficients of reactivity for the ZrC-moderated NVTR are summarized in Table 3). Thus, the overall power coefficient of reactivity for the ZrC NVTR is positive and this leads to an inherently unstable reactor. In going from cold, zero power to hot, full power this system is expected to undergo a reactivity increase of about 0.01 $\Delta k/k$.

The positive moderator and reflector temperature coefficients of reactivity for the ZrC NVTR are a consequence of the epithermal character of this reactor. The hard spectrum is also responsible for the relatively large critical mass of 175 kg for the reference ZrC-moderated NVTR. Thus, it is concluded that the ZrC-moderated NVTR possesses some very undesirable characteristics, namely its relatively large critical mass, large size (and hence, rather disappointing thrust-to-weight ratio of about 1 to 2), and its positive power coefficient of reactivity. The C-C composite based core described below eliminates most of the problems and offers enhanced performance.

Figure 5 shows k_{eff} versus F/M ratio (or versus FFD) for an NVTR with C-C composite fuel elements. A peak in the k_{eff} clearly occurs at an F/M value of about 3×10^{-4}. This behavior is quite different from that shown in Figure 2 for the ZrC system where k_{eff} increases continuously with increasing F/M. The first calculations performed on an NVTR using fuel elements made of C-C composite were for elements that included only a single fuel channel. The fuel channel radius was 0.55 cm and there were 32 coolant channels per element, each with a diameter of 0.096 cm; the element FFD was 2 cm. The 1800 MW core contained 7900 elements and had core dimensions of R=95 cm and H=150 cm with BeO reflector thicknesses of 15 cm. The thrust-to-weight ratio for this system was 2 and the critical mass was 40 kg.

In an effort to enhance the heat removal capabilities and reduce the reactor size, the C-C composite fuel elements were modified to include multiple fuel channels (see Figure 6). Current configurations include fuel elements with an FFD of ~2 to 3 cm and with from 12 to 32 fuel channels and a like range of coolant channels. From 2000 to 4000 of these elements are required for 1800 MW cores with dimensions of R=50 to 70 cm and H=150 cm. The critical mass is around 15 kg and thrust-to-weight ratios are in the range of 4 or 5-to-1.

Preliminary calculations show that both the moderator and reflector temperature coefficients of reactivity are negative for this C-C composite, thermal NVTR. The moderator temperature coefficient of reactivity, for example, has a value of about -1.5×10^{-5} $\Delta k/k$ per K. The overall power coefficient of reactivity is negative, the system is inherently stable, and in going from cold, zero power to hot, full power, the NVTR reactivity now decreases by about 0.02 $\Delta k/k$. Typical coefficients of reactivity for the C-C composite moderated NVTR are presented in Table 4. The focus of NVTR studies is now the multiple fuel channel, C-C composite fuel element which leads to a compact reactor with a negative power coefficient of reactivity, a low critical mass and high thrust-to-weight ratios. Calculations performed on the C-C composite NVTR have included a 3 mil ^{180}HfC protective liner for the hydrogen coolant channels.

Power density distribution calculations for the NVTR were performed in two dimensions with the DOT4 S_n transport theory code and in three dimensions with the MCNP Monte Carlo transport code. For the epithermal, ZrC-moderated NVTR the inherent axial power peaking factor (PPF) was 4.3 (see Figure 7). This large PPF leads to undesirable axial temperature profiles, including excessive wall temperatures at the core exit. For the thermal, C-C composite-moderated NVTR the inherent axial PPF was significantly lower at 2.9 (see Figures 8 and 9).

For both of these NVTRs, the radial and axial reflectors were BeO. An analysis of the flux distributions indicated that large differences in the neutronic properties of BeO and the adjacent graphite-moderated core region (either ZrC or C-C composite) was a significant contributor to the high power peaking. Thus, in the top axial reflector the first 10 cm of BeO adjacent to the core was replaced by C-C composite to provide a "buffer" (or better neutronic transition) between the core and the remaining 20 cm of BeO reflector. The bottom axial BeO reflector was completely replaced by C-C composite; although neutronically 10 cm of C-C followed by 20 cm of BeO is more desirable, the high temperatures at the core exit preclude the use of BeO. For the ZrC NVTR, the indicated axial reflector changes reduced the axial PPF from 4.3 to 2.3. For the C-C composite NVTR, these axial reflector changes reduced the axial PPF from 2.9 to 1.6. Calculations have shown that the 1.6 axial PPF in the C-C NVTR yields acceptable axial temperature profiles and wall temperatures at the core exit (see Figure 10).

The inherent radial PPF in the ZrC NVTR was 4.2; the corresponding value in the C-C NVTR was 3.3. For the C-C NVTR, the radial PPF is easily reduced by employing lower fuel loadings in the fuel elements on the core periphery (where the thermal flux peaks) as compared to the loadings in the central fuel elements. For example, the fuel elements in the outer 10 cm of the reference C-C NVTR core (core radius of 50 cm) were loaded with 60 atm of UF_4 and 40 atm of He while the fuel elements in the inner 40 cm of the core were maintained at the nominal 100 atm UF_4 loading. This change reduced the radial PPF from 3.3 to 1.6 for the C-C NVTR. The 1.6 radial PPF leads to good radial temperature distributions. The cost of this reduced fuel loading in the peripheral elements is a 14% overall reduction in UF_4 relative to the case where all elements are at the nominal UF_4 loading of 100 atm. This reduction does not pose any concerns with regard to criticality for the C-C NVTR. The reactivity loss is easily compensated for by small increases (~5%) in the core size, fuel enrichment, or nominal fuel operating pressures.

Typical reactor characteristics for the ZrC-moderated and C-C composite moderated NVTRs are summarized in Table 5.

4.0 THERMO-MECHANICAL ANALYSIS

Thermo-mechanical studies carried out at Los Alamos on a solid fuel Rover reactor indicate that the stress in the fuel element material limits the power density achievable in the reactor. It was also concluded that most of the fuel failures were due to damage of the

protective coating on the coolant channel surface and subsequent migration of hydrogen into the graphite matrix.[8] The fuel element structural material in the NVTR is exposed to high temperatures at the fuel and coolant channels. The difference in temperature between the coolant channel surface and the fuel channel surface leads to thermal stress in this structural material that has to be maintained below a certain limiting value to ensure the integrity of the coating and the structural material.

In view of this susceptibility of the fuel element to failure and to maximize power density, thermo-mechanical studies were performed on NVTR fuel elements. Two-dimensional finite element analyses (FEM) have been carried out on NVTR fuel elements to evaluate and improve the fuel element design so that higher power density can be achieved.

Thermo-mechanical calculations were performed on the NVTR fuel elements using the ANSYS 4.4 finite element code[9]. ANSYS can handle both 2-D and 3-D thermal and stress analyses. The first calculations were performed on the original ZrC fuel element containing a single fuel channel (see Figure 1). The fuel channel radius was 1.0865 cm and the fuel element flat-to-flat distance was 3.272 cm. The fuel element contained 32 coolant channels, each with a diameter of 0.142 cm. Coolant channel-to-coolant channel web thickness was 0.15 cm and coolant channel-to-fuel channel web thickness was 0.04 cm. For a fuel heat generation rate of 800 w/cc, hydrogen exit temperatures of 3100 K, and maximum exit wall temperatures of 3300 K, the maximum thermal stress was calculated as 54.5 MPa. At 2900 K the ZrC fracture stress is only about 31 MPa. At 2000 K, the ZrC fracture stress is about 50 MPa. Obviously, operation at temperatures of 3000 K or above is not possible with such ZrC elements and even operation at 2000 K will require the use of carefully designed multiple fuel channel elements. In addition to poor thermal mechanical performance, as indicated above, the use of Zr-C fuel elements introduces a number of other serious problems. These include relatively large critical mass because of the epithermal neutron spectrum, a physically large reactor with poor specific impulse, poor power peaking distributions, and an overall positive power coefficient of reactivity.

Calculations were performed next on multiple fuel channel elements. The following fuel element designs were examined:

1. Two designs (Designs I and II) with alternate rings of fuel and coolant channels (see Figure 6) with Design II having a larger number of smaller fuel and coolant channels than Design I;

2. A design using a square lattice (Design III), in which each fuel channel is surrounded by four coolant channels and vice versa.

The analyses employ four-noded isoparametric thermal elements and plain strain elements for the thermal and stress analyses, respectively. These analyses are carried out at the mid-section of the core. A 1/12th symmetry is considered for the first two designs and a square lattice with four coolant channels and one fuel channel is considered for the third design.

Uniform volumetric heat generation is assumed in the fuel channel. A coolant

temperature of 3000 K and a constant wall-to-coolant heat transfer coefficient are used as boundary conditions for the thermal analyses. Symmetric displacement constraints have been imposed at the boundaries for the stress analyses. The three fuel element designs were analyzed for a fuel volumetric heat generation rate of 6550 w/cc. The fuel element geometry design parameters considered for these studies are presented in Table 6. The temperatures generated by thermal analyses have been used as input for the stress analysis.

For comparison purposes, graphite, zirconium carbide and carbon-carbon (C-C) composite were selected as materials for the fuel element structure. The properties of graphite used in the analyses are the same as those reported in Reference 10. Zirconium carbide[11] and carbon-carbon composite properties as reported in the literature[12,13,14] are used. The properties of C-C composite vary based on the type of preform and the type of manufacturing process. Thus, there is wide range in the properties of C-C composites. To overcome this difficulty, the most probable values of the relevant properties are selected and used for the analyses. Some properties used for these parametric studies are presented in Table 7. A reference temperature of 3000 K is applied for the evaluation of fuel element structural material properties.

The FEM analyses generate the temperature, component stress and principal stress at the nodes. Stress intensity is used as a parameter for optimization studies.

The temperature distributions in the three fuel element designs for the case in which graphite is the fuel element structural material are presented in Figure 11. The temperature distribution is strongly dependent on the arrangement of fuel and coolant channels. In the first design, the peak temperatures were observed to occur in the web region between the fuel channels. The peak temperature in the second design occurs at the first ring of fuel channels. In the third design, the peak temperatures are symmetric and the temperature distribution is relatively uniform around the fuel and the coolant channels. The maximum temperatures and the heat fluxes for the three designs in which graphite is the structural material are presented in Table 8.

The stress contours for the three designs for the case in which graphite is the fuel element structural material are presented in Figure 12. Stress values were found to be strongly dependent on the temperature distribution in the fuel element. In the first design the maximum stress is observed at the web region between the coolant and the fuel channel and it occurs on the surface of the coolant and the fuel channels. In Design II the maximum stress is observed in the web region between the second ring fuel channels. The stress intensity in Design II is the highest of the three designs. The square lattice design (Design III) gives a lower stress in the fuel element material than the annular fuel/coolant channel designs (Design I and II). The

The excellent behavior of this material is due to its lower coefficient of thermal expansion (CTE) and relatively lower Young's modulus. The stress in C-C composite is lower than its strength even at a power density of 12000 w/cc as seen in Figure 13. The stress intensity at the interface between the C-C composite and the HfC coating is about three times higher than the stress in the C-C composite; however, it is still much lower than the strength of the HfC coating material. Thus, thermal stress is not a limitation for achieving high power density in the high temperature NVTR when fuel elements are employed using C-C composite for the structural material.

5.0 SUMMARY AND CONCLUSIONS

The use of C-C composite fuel elements in the NVTR leads to a compact reactor with low critical mass, good power peaking characteristics, an overall negative power coefficient of reactivity and, hence, good stability, and a propulsion system with high specific impulse. Thermo-mechanical analysis has shown excellent thermo-mechanical behavior under the high power density, high temperature NVTR environment.

Thermal analyses and engine balance calculations on the NVTR have been performed in cooperation with Rocketdyne Division, Rockwell International. The NVTR core is integrated into an 75 k lb_f engine design using an expander cycle and dual turbopumps as shown in Figure 14. The assumptions used in the analysis and system balance are shown in Table 10. Thermal analysis performed by the University of Florida[15] for the fuel element has included heat transfer in fissioning gases via molecular and electron thermal conduction, radiative heat transfer, and energy transport by fission fragments. For an exit coolant (propellant) temperature of 3100 K, the maximum moderator temperature is 3300 K. Within the fuel channel, the exit fuel gas temperature rises rapidly from 3300 K at the wall up to a centerline value of about 4600 K (see Figure 10). The fuel centerline peak temperature is a function of the photon absorption cross section and was estimated for UF_4 from data available for uranium and UF_6. With hydrogen at $10x10^6$ pascals and a nozzle expansion ratio of 1:500, a specific impulse of 1000 s can be attained. The hydrogen pressure drop across the core is from 20 to 200 psi, depending upon the selected number and size of coolant channels employed in the fuel element design. The thrust is 75,000 lbs. with a hydrogen flow rate of 30 kg/s and a reactor thermal power of 1800 MW. Typical NVTR design and performance parameters are summarized in Figure 15.

A significant technology development opportunity is afforded by the NVTR. The NVTR concept has the characteristic that it is based on modest extrapolations of technology, yet it is a gas/vapor core reactor. It shares some GCR critical issues, such as criticality and reactor control, fuel mobility and handling, radiative heat transfer, and high temperature materials compatibility. It presents the opportunity to address GCR issues within a framework through which advances in technology can be incorporated, and experience gained, in a small stepwise manner. In addition to the incremental approach to technology development, the NVTR offers another advantage in the initial cost of development. Since the fuel for the NVTR is readily available, the initial efforts will not require major expenditures in fuel development. This affords an opportunity to develop technology supporting a nuclear concept

wherein the bulk of the technology developed will be applicable to and draw from parallel efforts in related fields that are non-nuclear in nature, for example, composite material analysis, design, and fabrication. The costs of the initial research will thus not have to bear the extra cost associated with nuclear component development and furthermore, will be borne by a variety of programs, minimizing the cost to each other.

ACKNOWLEDGMENTS

This work was performed for the Ballistic Missile Defense Organization, Innovative Science and Technology Directorate, under contract NAS3-26314 managed by NASA's Lewis Research Center. Portions of the work have been performed under NASA Grant NAG3-1293 from the Office of Nuclear Propulsion, NASA Lewis Research Center. Neutronics calculations were performed in part with the support of the National Science Foundation and the San Diego Supercomputer Center and by the University of Florida and the IBM Corporation through the Research Computing Initiative at the University of Florida. Thermal analysis and engine balance calculations for this concept were performed with Rocketdyne Division, Rockwell International under a Teaming Agreement.

REFERENCES

1. Diaz, N.J. and E.T. Dugan, Heterogeneous Gas Core Reactor Power Plants, Disclosure of Invention, University of Florida, Gainesville, FL., 1977.

2. Han, K.I., "Heterogeneous Gas Core Reactor," Ph.D. Dissertation, University of Florida, Gainesville, FL., 1977.

3. Kerrick, W.E., "Graphite-Moderated, Uranium Hexafluoride-Fueled Unit Cells: Neutronic Analysis with Application to Fission-Fusion Blankets," Masters Project, University of Florida, Gainesville, FL., 1978.

4. Kahook, S.D., "Neutronic Analysis of Highly Enriched Graphite and Beryllium Moderated Heterogeneous Gas Core Reactors," Masters Project, University of Florida, Gainesville, FL., 1986.

5. Greene, N.M., J.L. Lucius, L.M. Petrie, W.E. Ford, III, J.E. White, and R.Q. Wright, "AMPEX: A Modular Code System for Generating Coupled Multigroup Neutron-Gamma Libraries from ENDF/B," ORNL-TM-3706, Oak Ridge National Laboratory, Oak Ridge, TN., 1982.

6. Rhoades, W.A. and R.L. Childs, "An Update Version of the DOT-4 One- and Two-

7. Breismeister, J.F., Editor, "MCNP-A General Monte Carlo Code for Neutron and Photon Transport," Version 3A, LA-7396, Rev. 2, Los Alamos National Laboratory, Los Alamos, NM., 1986.

8. Lawton, R.G. and W.R. Prince, "Rover Graphite Fuel Element Thermal Stress Experiments and Analyses," LA-3849-MS, Los Alamos National Laboratory, Los Alamos, New Mexico., 1968.

9. Desalvo, J.D. and Gorman, R.W., "ANSYS4.4, A Generalized Finite Element Computer Code for Thermal and Stress Analysis," Swanson Analysis, Inc., Houston, PA., 1989.

10. Rowley, J.C., W.R. Prince and R.G. Gido, "A Study of Power Density and Thermal Stress Limitations of Rover Reactor Fuel Element," LA-3323-MS, Los Alamos National Laboratory, Los Alamos, New Mexico., 1965.

11. Battelle Columbus Laboratories, "Engineering Property Data on Selected Ceramics Volume 2 Carbides," MCIC-HB-07, Volume 2, Materials and Ceramics Information Center, Battelle Columbus Laboratories, Columbus, OH, August, 1979.

12. Hsu, S.E. and C.I. Chen, "The Processing and Properties of Some C-C Systems,"

[redacted]

Press, Inc., Boston, p. 721-749., 1989.

13. McAllister, E.L. and A.R. Taverna, "A Study of Composition-Construction Variation in 3D C-C Composites," Proceedings of 1975 ICCM, Scala E., Anderson E., Troth I.,

Table 1. Typical NVTR Atom Densities

N^{U235}	= 1.835×10^{20}	Atoms/cc	UF_4 gas at 100 atm and 4000 K
N^{F19}	= 7.34×10^{20}	Atoms/cc	
N^{H}	= 7.34×10^{20}	Atoms/cc	H gas at 100 atm and 2000 K
N^{Zr}	= 3.9×10^{22}	Atoms/cc	
N^{C12}	= 3.9×10^{22}	Atoms/cc	ZrC at 2000 K
N^{C12}	= 8.5×10^{22}	Atoms/cc	C-C composite at 2000 K
N^{Be}	= 7.2×10^{22}	Atoms/cc	BeO at 1200 K
N^{016}	= 7.2×10^{22}	Atoms/cc	

Table 2. Percentage of Fissions By Energy for Reference NVTR's

Energy Range	Percent Fissions in ZrC NVTR	Percent Fissions in C-C NVTR
15 MeV to 0.821 MeV	1.5	0.2
0.82 MeV to 5.53 keV	10.3	0.8
5.53 keV to 1.86 eV	45.0	12.2
< 1.86 eV	43.2	86.8

Table 3. Reactivity Coefficients for
ZrC-Moderated NVTR

$\alpha^{U233}(T)$	-2×10^{-7} $\Delta k/k$ per °K	(300 K to 3000 K)
$\alpha^{H}(P)$	$+4.9\times10^{-4}$ $\Delta k/k$ per atm	(0 to 100 atm)
$\alpha^{C12}(T)$	$+2\times10^{-6}$ $\Delta k/k$ per °K	(800 K to 1600 K)
$\alpha^{H}(T)$	$+2\times10^{-7}$ $\Delta k/k$ per °K	(300 K to 3000 K)
$\alpha^{BeO}(T)$	$+2\times10^{-5}$ $\Delta k/k$ per °K	(600 K to 1200 K)

Table 4. Reactivity Coefficients for
C-C Composite Moderated NVTR

$\alpha^{U233}(T)$	-2×10^{-7} $\Delta k/k$ per °K	(300 K to 3000 K)
$\alpha^{H}(P)$	$+4.9\times10^{-4}$ $\Delta k/k$ per atm	(0 to 100 atm)
$\alpha^{C12}(T)$	-5×10^{-5} $\Delta k/k$ per °K	(800 K to 1600 K)
$\alpha^{H}(T)$	$+2\times10^{-7}$ $\Delta k/k$ per °K	(300 K to 3000 K)
$\alpha^{BeO}(T)$	-5×10^{-5} $\Delta k/k$ per °K	(600 K to 1200 K)

Table 5. Typical NVTR Reactor Characteristics

	ZrC Moderated NVTR	C-C Moderated NVTR
Core Size		
R (m)	1.2	0.5
H (m)	1.3	1.5
Vol (m^3)	5.9	1.2
Critical Mass		
U^{233} (kg)	175	30
Power Coefficient of Reactivity	+	-
Maximum Axial PPF	2.2	1.5
q″ (W/cm^2)	~300	~600
Thrust-to-Weight Ratio	~1	~5

Table 6. Fuel Element Design Variables for Thermo-Mechanical Studies

Type of Design	Number of Coolant Channels	Number of Fuel Channels	Coolant Channel Diameter (cm)	Fuel Channel Diameter (cm)	Element Flat-to-Flat Size (cm)	Lmin[a]
DESIGN-I	24	13	0.268	0.364	3.9317	0.2559
DESIGN-II	43	24	0.200	0.267	3.9317	0.208
DESIGN-III	83	64	0.144	0.16	4.9736	0.243

[a]Minimum distance between fuel and coolant channels in cm.

Table 7. Comparison of Fuel Element Structural Material Properties

Material	Thermal Conductivity (w/m/K)	Youngs Modulus (GPa)	C.T.E. (m/m)	Density (Kg/m3)	Yield Strength (MPa)	(Type) Reference
Graphite	30.0 (@ 2600 K)	14.63 (@ 2317 K)	4.968e-6 (@ 2317.0 K)	1800 (@ 3000 K)	26.0 (@ 3000 K)	(ATJ-S) Rowely 1965
Zirconium Carbide	43.28 (@ 2500 K)	344 (@ 1505 K)	8.3e-6	6560	48.0 (@ 1999 K)	MCIC report 1979
Carbon/Carbon Composite	77.89 (@1140 K)	55.87 (@1921 K)	1.1e-6 (@ 3033 K)	1800 (@ 1921 K)	99.31 (@ 1921 K)	(3-D) McAllister 1975
Hafnium Carbide	38.08 (@ 2500 K)	296.09	7.2e-6	12670	101.99 (@ 2500 K)	MCIC report 1979

Table 8. Maximum Temperatures, Stresses and Heat Flux in the Three Fuel Element Designs. (Heat flux normalized to the heat flux in Design-I; graphite is the fuel element structural material.)

Type of Design	Normalized Heat Flux In Coolant Channel	Normalized Heat Flux In Fuel Channels	Maximum Stress Intensity (MPa)	Maximum Temperature (K)
DESIGN-I	1.000	1.000	27.91	3161
DESIGN-II	0.75	0.74	37.26	3200
DESIGN-III	0.54	0.45	25.10	3230

Table 9. Variation in Fuel Element Design III Maximum Stress with Fuel Element Structural Material

Material Type	Stress at the Coating and Fuel Element Interface (MPa)	Stress in Fuel Element Material (MPa)	Temperature (K)	Power (W/CC)
GRAPHITE	32.36	26.97	3193	6550
ZIRCONIUM CARBIDE	987.85	388.81	3167	6550
CARBON/CARBON COMPOSITE	20.80	6.44	3270	12000

Table 10. Assumptions Used in NVTR Rocket Engine System Balance

Thrust Level	75,000	lb_f
Chamber Pressure	1,500	psia
Nozzle Area Ratio	500:1	--
Nozzle Percent Length	130	--
Turbine Speed	90,000	RPM
Turbine Admission	1.0	--
Turbine Pitch Line Velocity	1,650	ft/s
Turbine Type	50% Reaction	--
Turbine Bypass Fraction	0.10	--
Number Of Turbine Stages	2	--
Number of Pump Stages	3	--

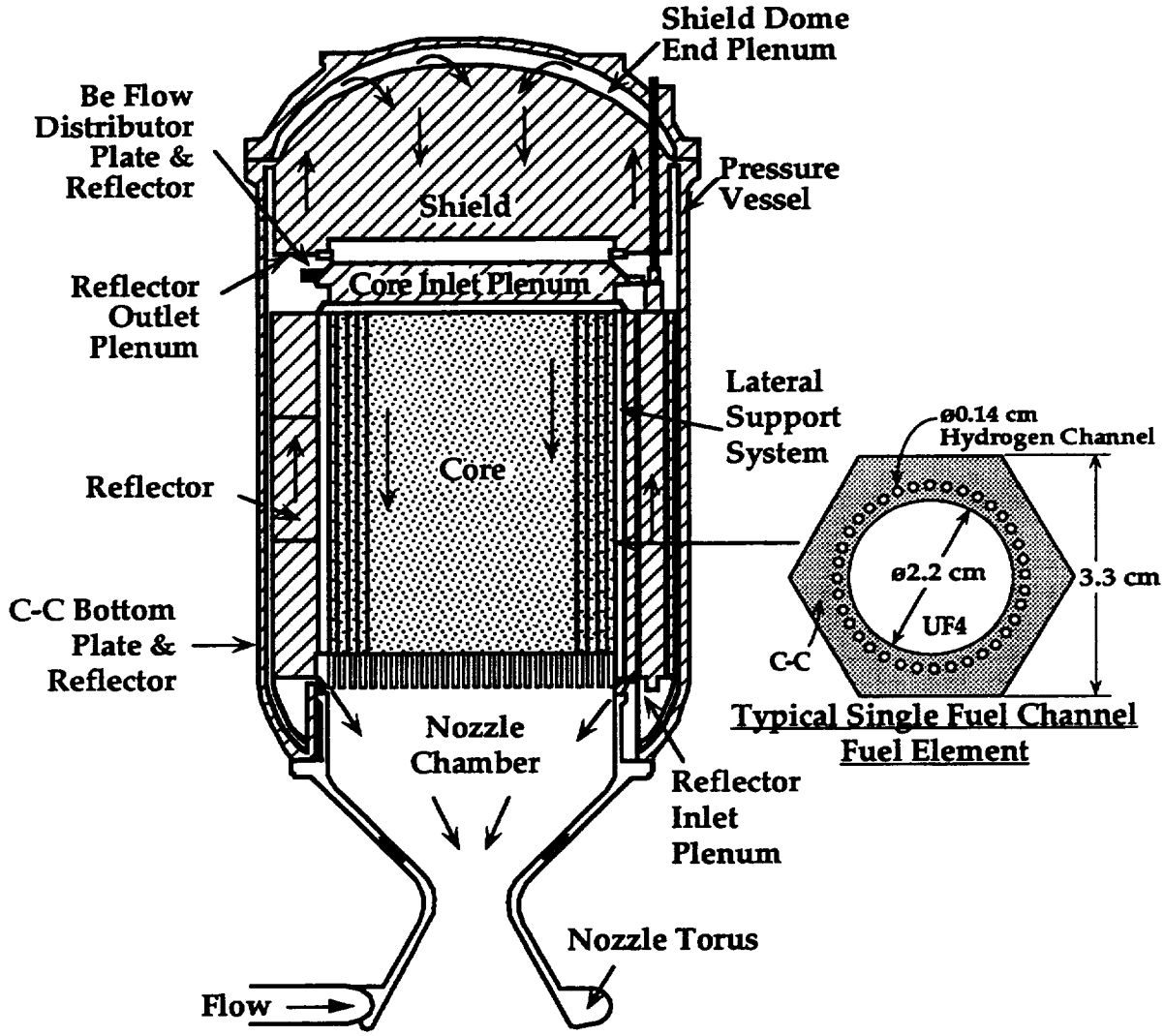

Fig. 1. Side view of conceptual nuclear vapor thermal rocket engine.

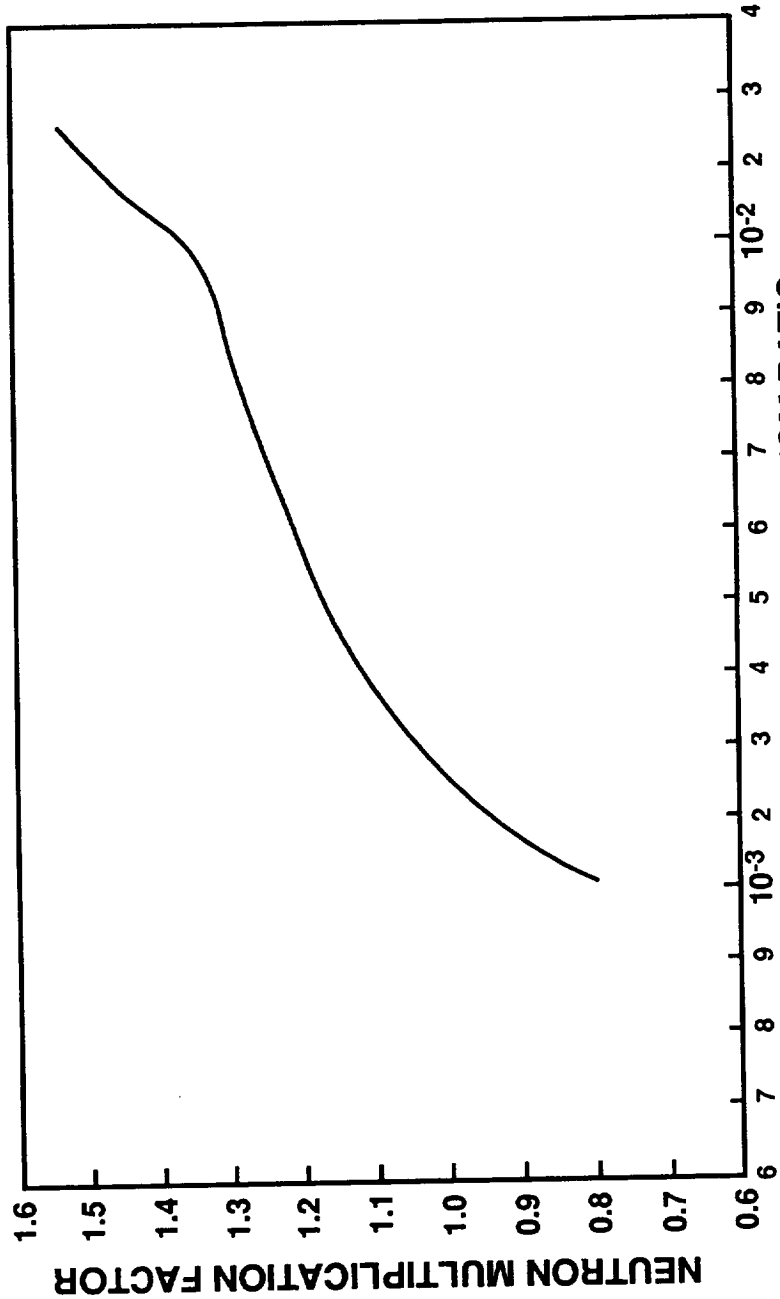

Fig. 2. Neutron multiplication factor versus fuel-to-moderator atom ratio for the ZrC - moderated NVTR.

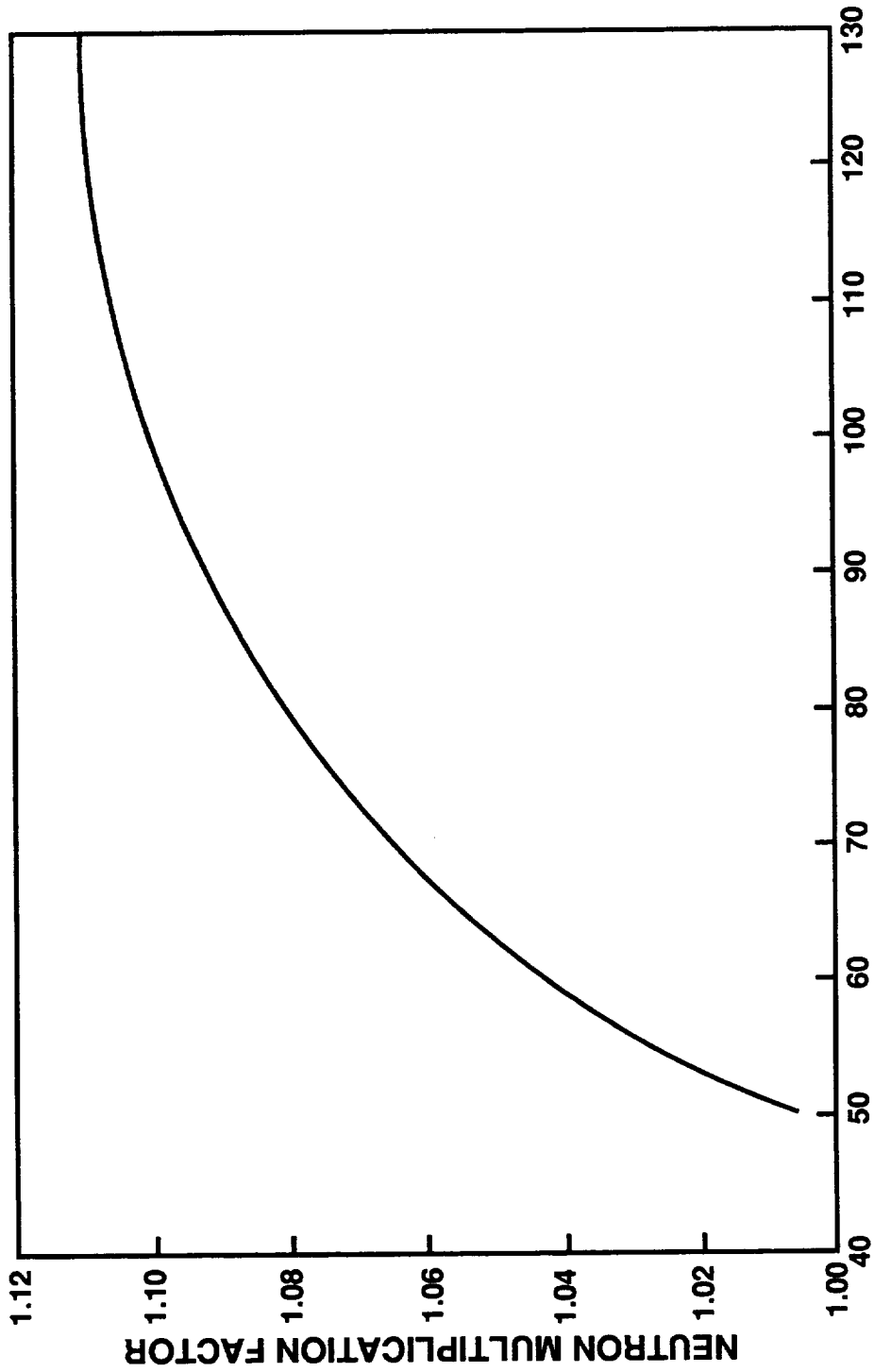

Fig. 3. Neutron multiplication factor versus core radius for the ZrC - moderated NVTR.

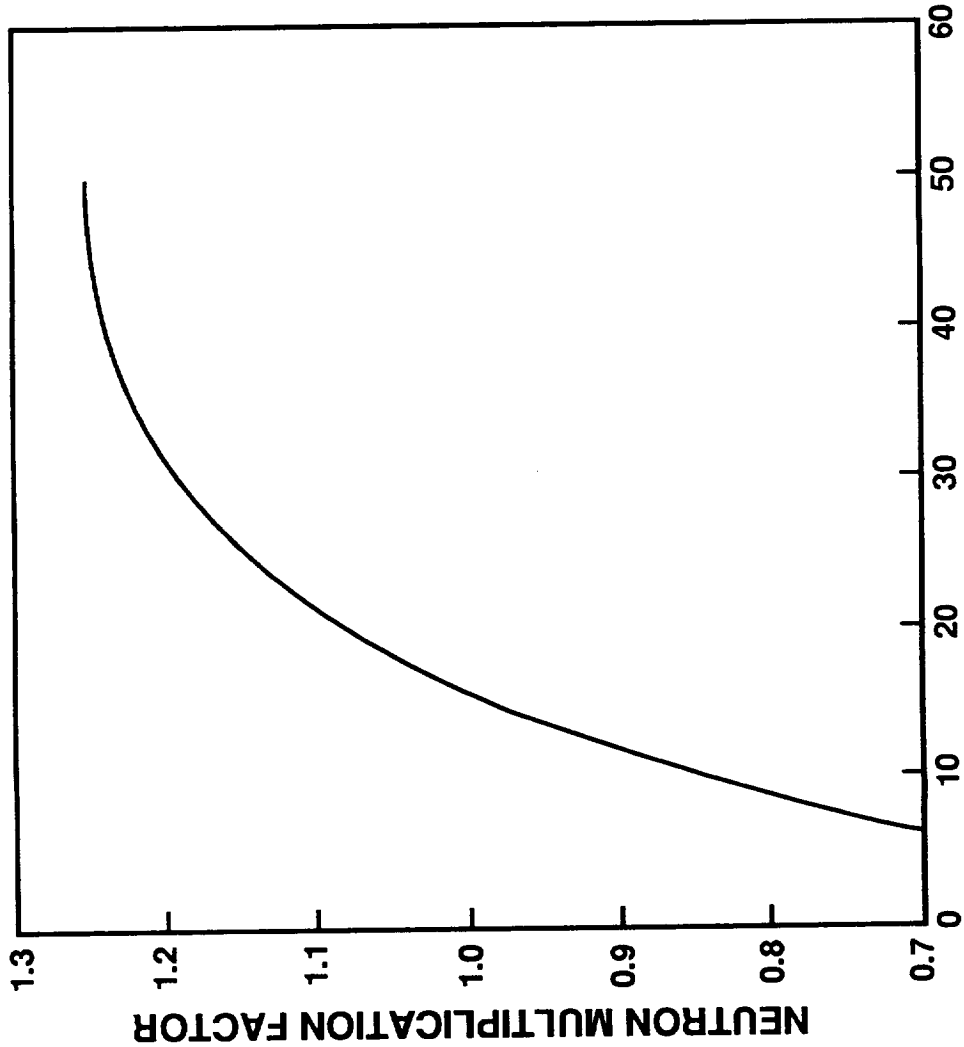

Fig. 4. Neutron multiplication factor versus reflector thickness for the ZrC - moderated NVTR.

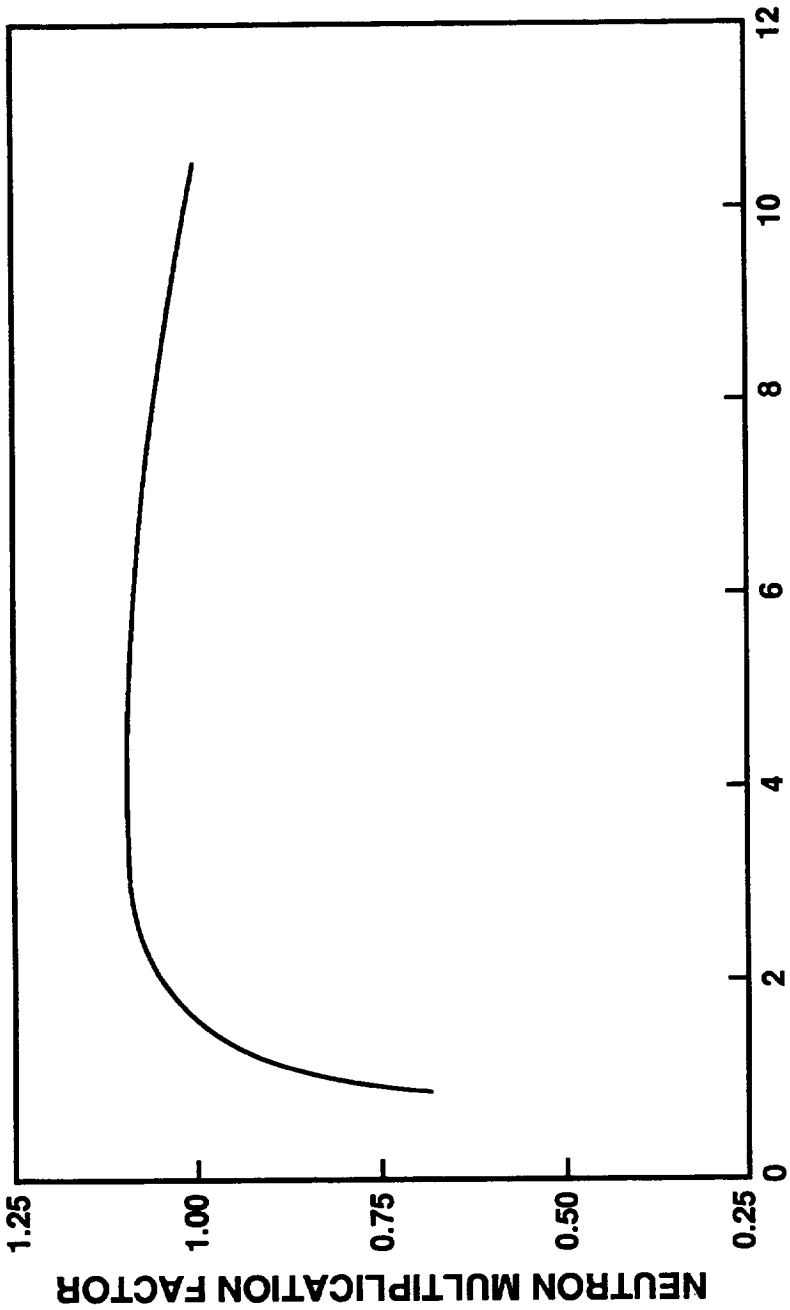

Fig. 5. Neutron multiplication factor versus fuel-to-moderator atom ratio for the C-C composite - moderated NVTR.

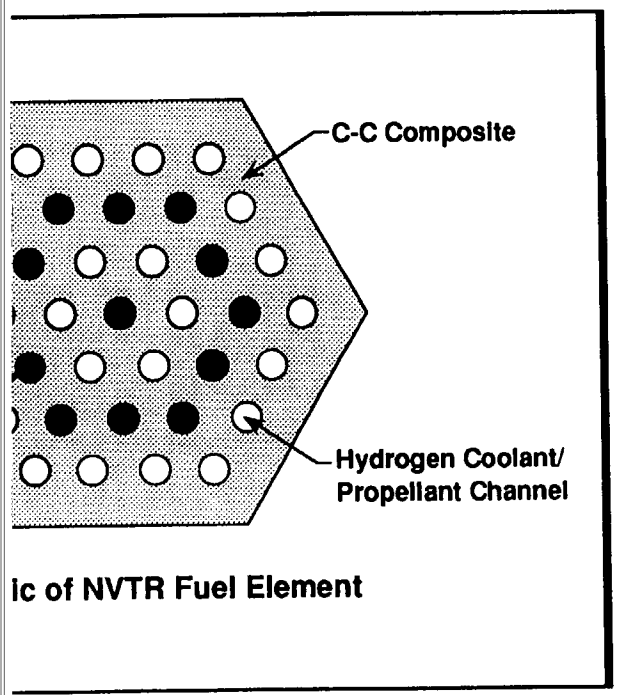

ic of NVTR Fuel Element

and multiple fuel channel

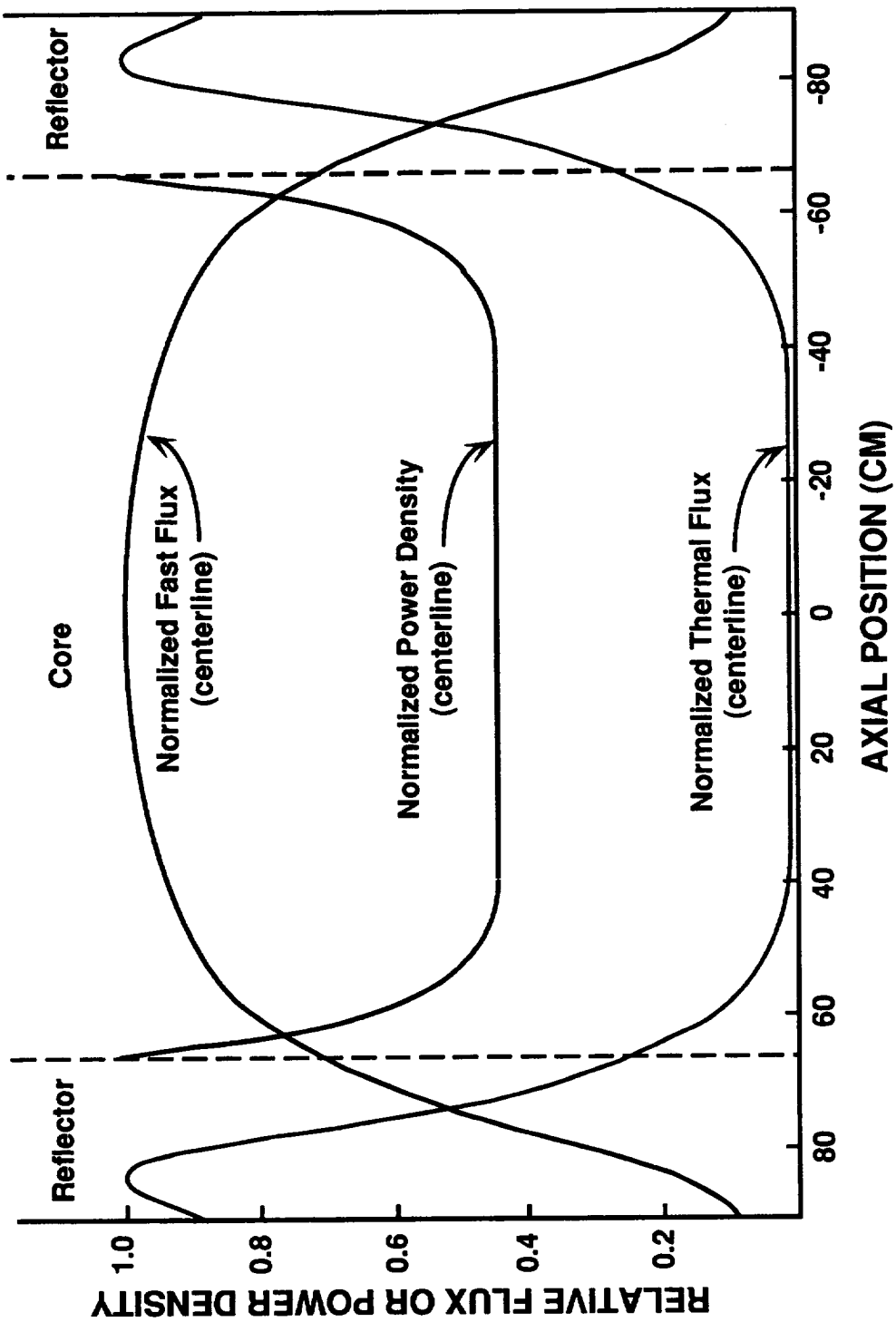

Fig. 7. Axial centerline flux and power density profiles in ZrC - moderated NVTR.

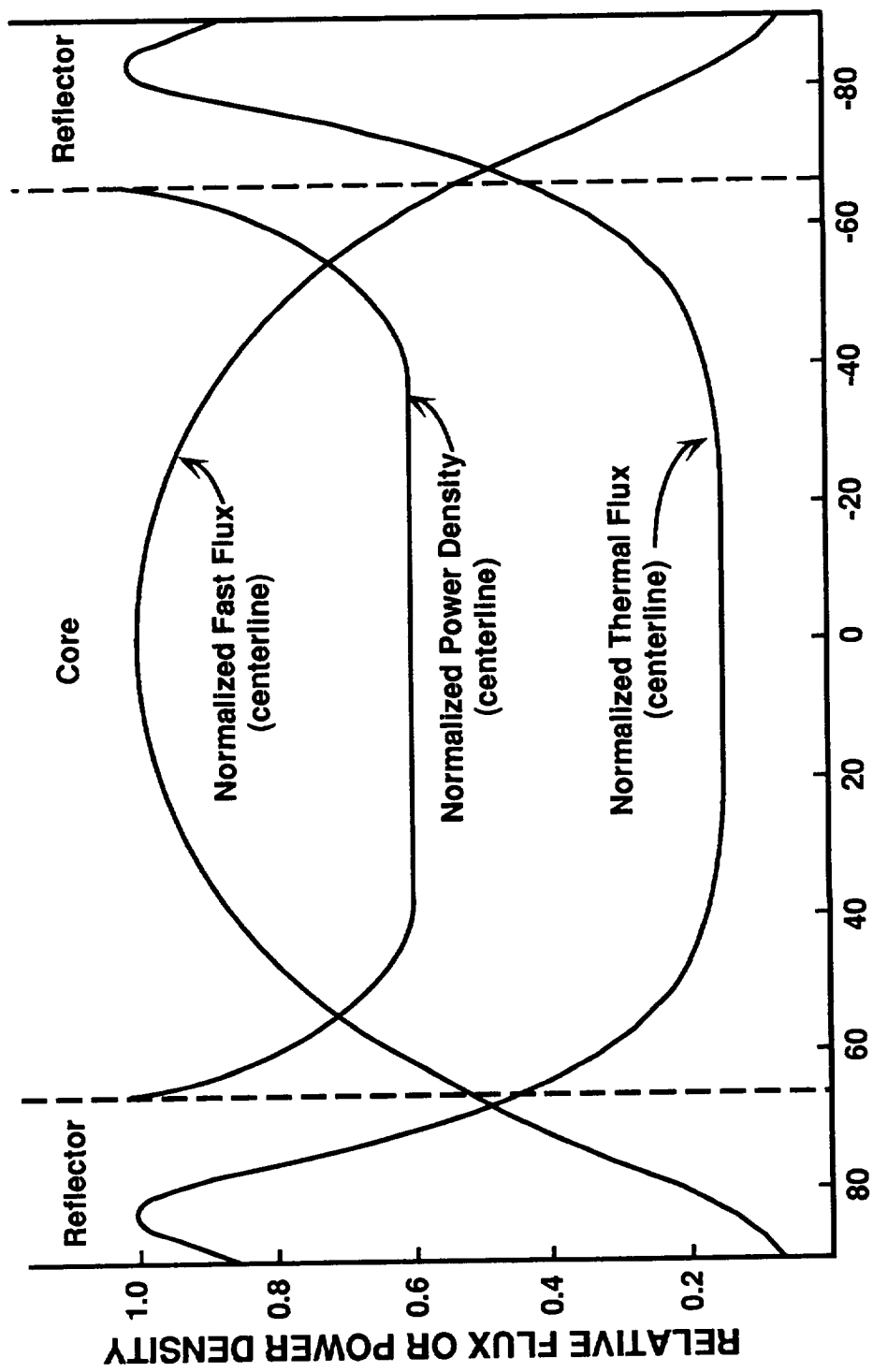

Fig. 8. Axial centerline flux and power density profiles in C-C composite - moderated NVTR.

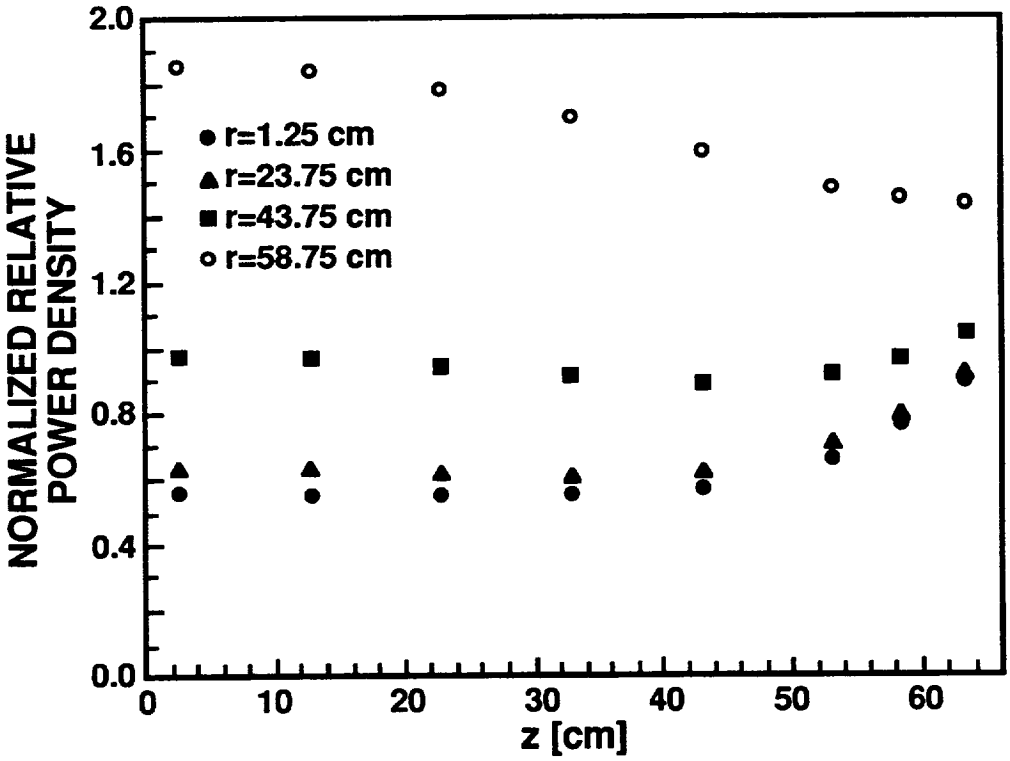

Fig. 9. Axial power density profiles at different radial positions in C-C composite - moderated NVTR.

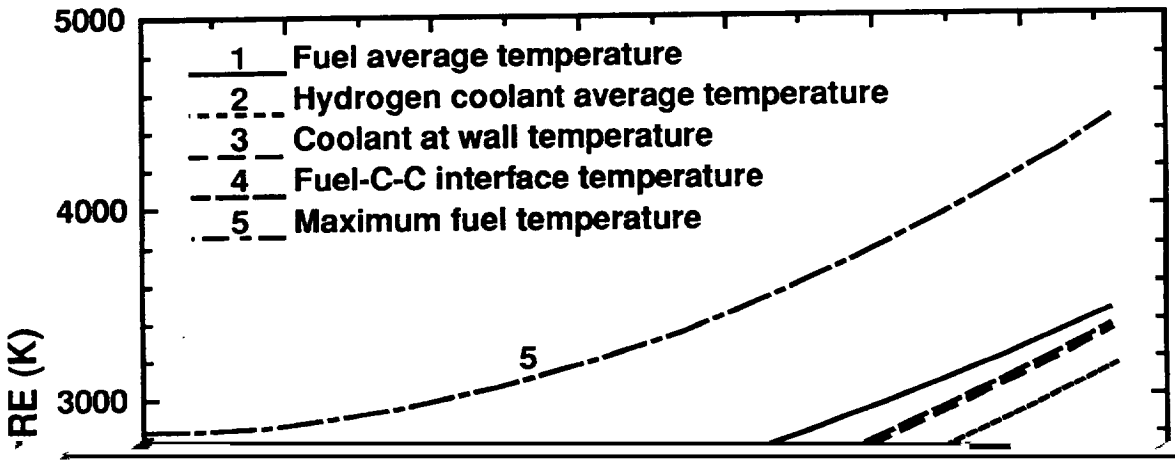
5000
4000
3000
RE (K)
1 Fuel average temperature
2 Hydrogen coolant average temperature
3 Coolant at wall temperature
4 Fuel-C-C interface temperature
5 Maximum fuel temperature
5

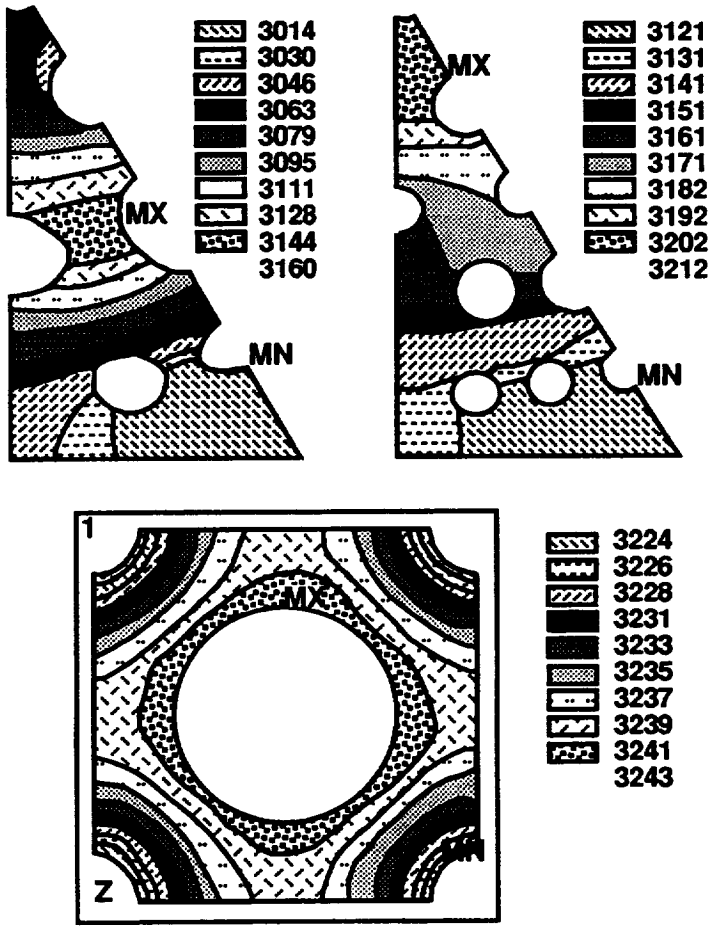

Fig. 11. Temperature distribution in the three fuel element designs (K).

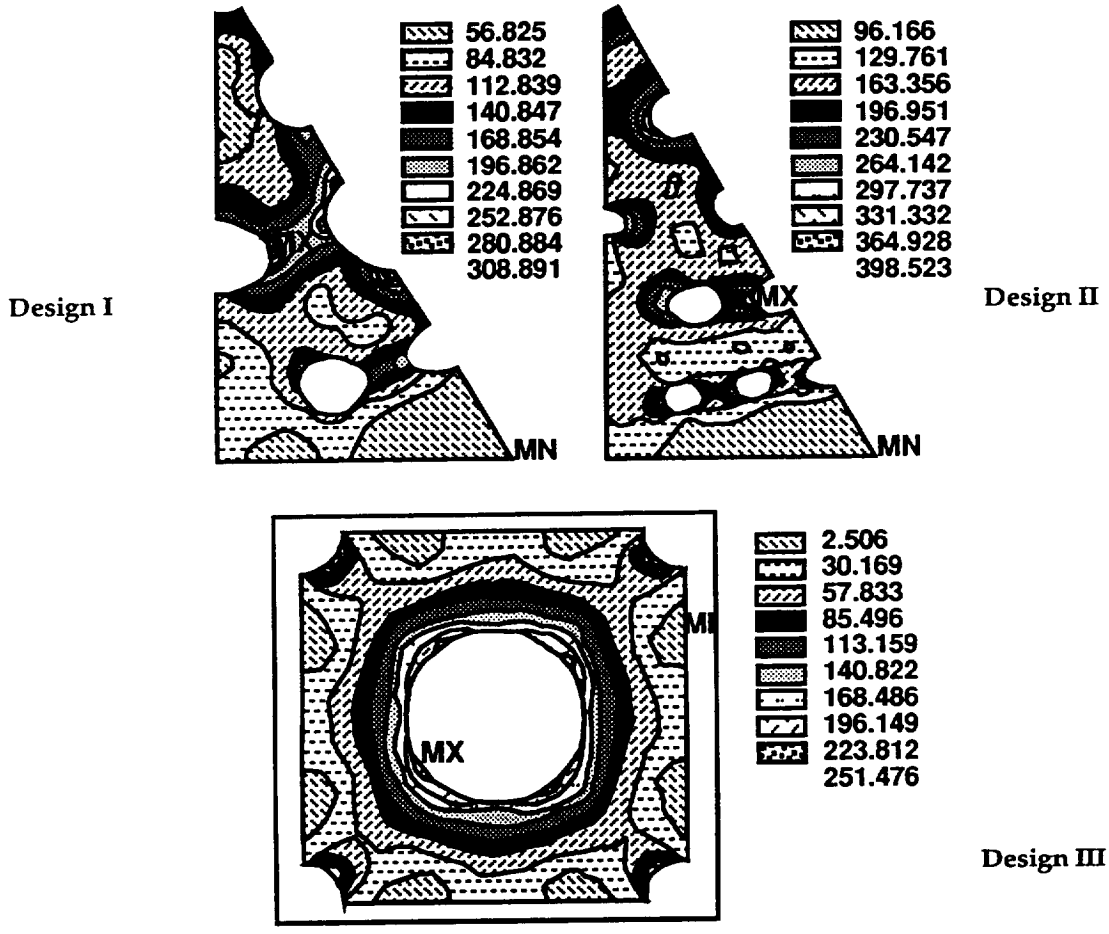

Fig. 12. Stress distribution in the three fuel element designs (units are *0.9807e5 Pa).

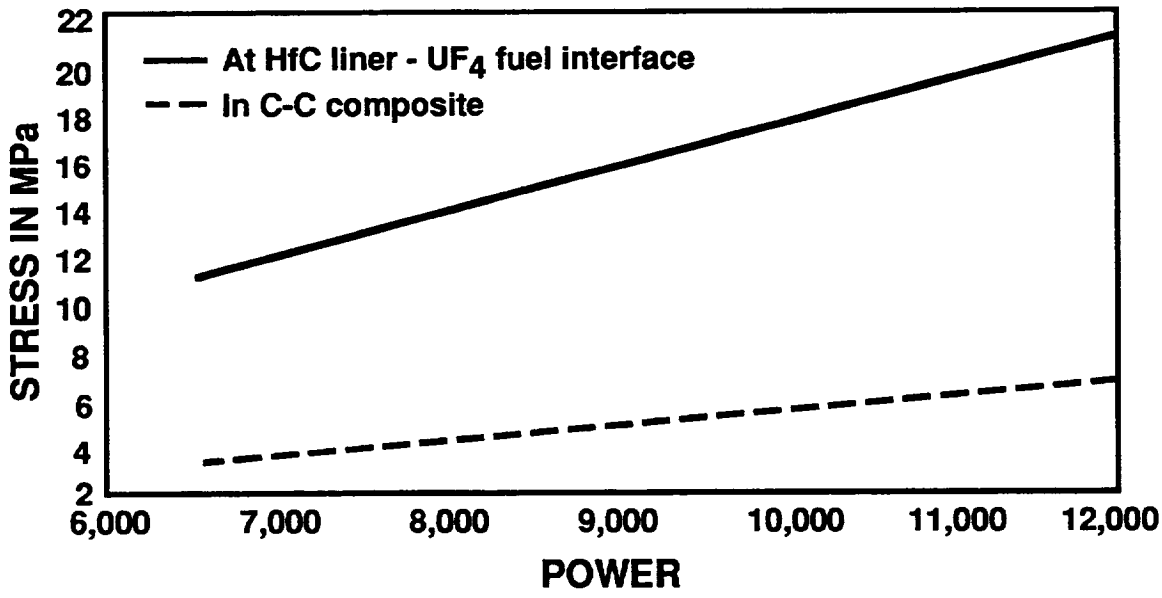

Fig. 13. Maximum stress in design III fuel element as a function of power density for C-C composite.

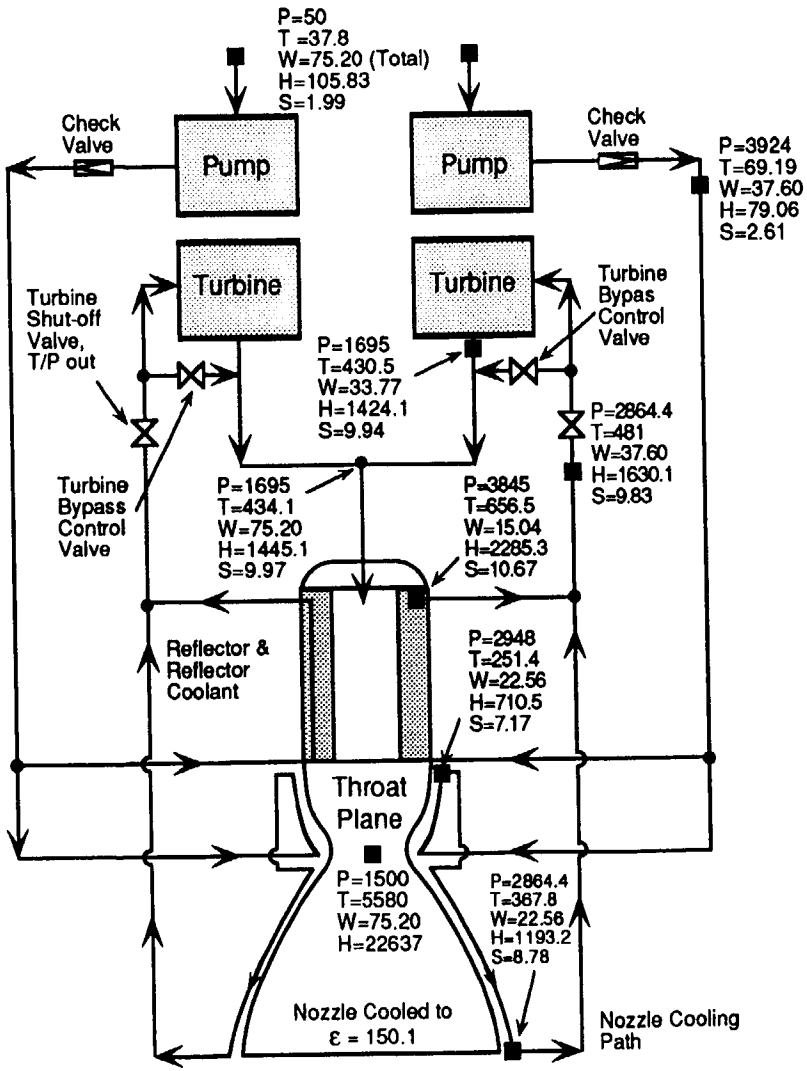

Design Values

Pump Flowrate (Total)	75.20	lb_m/s
Pump Discharge Pressure	3,924	psia
Pump Efficiency (%)	80.01	- - -
Turbopump RPM	70,000	RPM
Turbopump Power (Each)	9,836	HP
Turbine Inlet Temperature	481	Deg-R
Turbine Pressure Ratio	1.69	- - -
Turbine Flow Rate (Each)	33.77	lb_m/s
Reactor Thermal Power	1,769	MW
Fuel Element and Reflector Power	1,716	MW
Nozzle Chamber Temperature	5,580	deg-R
Chamber Pressure (Nozzle Stagnation)	1,500	psia
Nozzle Expansion Area Ratio	500:1	- - -
Vacuum Specific Impulse (Delivered)	997.8	sec

Heat loads are as follows:

Nozzle-con (total):	30.05	MW
Nozzle-div (total):	22.97	MW
Reflector (total):	35.00	MW

P = psia
T = deg-R
W = lb_m/s
H = BTU/lb_m
S = BTU/lb_m-R

Note: Flowrates indicated are for one-half of system

Fig. 14. Representative NVTR engine system balance.

Nozzle Area Ratio	500
Fuel Pressure	100 atm
Average Fuel Temperature	4000 K
Maximum Element Heat Flux	420 W/cm^2
Nominal Element Length	150 cm
Fuel Volume Fraction	0.15
Coolant Volume Fraction	0.15
Moderator Volume Fraction	0.70
Fuel Element Power	0.9 MWt
Element Heat Transfer Area	2141 cm^2
Reactor Core L/D	1.5
Fuel Channel Diameter	0.142 cm
Fuel Channel Sectional Area	0.0158 cm^2
Total Fuel Channel Area Per Element	0.505 cm^2
Fuel Element Sectional Area	3.464 cm^2
Element Diameter (across flats)	2.2 cm
Coolant Channel Diameter	0.142 cm
Coolant Channel Sectional Area	0.0158 cm^2
Total Coolant Channel Area Per Ele.	0.505 cm^2
Core Volume	1.2 m^3
Core Power Density	1500 MW/m^3
Fuel Element Mass, Total	1.35 MT
Forward Reflector Mass	0.60 MT
Aft Reflector Mass	0.51 MT
Radial Reflector Mass	2.47 MT
Radiation Shield Mass	0.90 MT
Total Reactor Mass	5.83 MT
Misc. Engine Components Mass	0.9 MT
Total Engine Mass	6.83 MT
Engine F/W	5.0

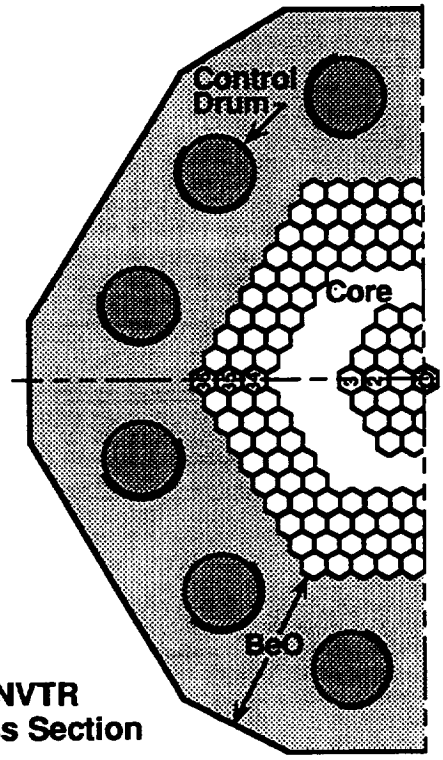

NVTR
Cross Section

Fig. 15. Typical NVTR engine parameters.

REPORT DOCUMENTATION PAGE

Form Approved
OMB No. 0704-0188

1. AGENCY USE ONLY (*Leave blank*)	2. REPORT DATE	3. REPORT TYPE AND DATES COVERED
	April 1996	Final Contractor Report

4. TITLE AND SUBTITLE

Conceptual Design of a Vapor Core Reactor Rocket Engine for Space Propulsion

5. FUNDING NUMBERS

WU-233-01-0N
C-NAS3-26314

6. AUTHOR(S)

E.T. Dugan, N.J. Diaz, S.A. Kuras, S.P. Keshavmurthy, and I. Maya

7. PERFORMING ORGANIZATION NAME(S) AND ADDRESS(ES)

University of Florida
Ultrahigh High Temperature Reactor and Energy Conversion Program
Innovative Nuclear Space Power and Propulsion Institute
Gainesville, Florida 32611

8. PERFORMING ORGANIZATION REPORT NUMBER

E-9881

9. SPONSORING/MONITORING AGENCY NAME(S) AND ADDRESS(ES)

National Aeronautics and Space Administration
Lewis Research Center
Cleveland, Ohio 44135-3191

10. SPONSORING/MONITORING AGENCY REPORT NUMBER

NASA CR-198388

11. SUPPLEMENTARY NOTES

Project Manager, Harvey S. Bloomfield, Power Technology Division, NASA Lewis Research Center, organization code 5440, (216) 433-6131.

12a. DISTRIBUTION/AVAILABILITY STATEMENT

Unclassified - Unlimited
Subject Category 20

This publication is available from the NASA Center for Aerospace Information, (301) 621-0390.

12b. DISTRIBUTION CODE

13. ABSTRACT (*Maximum 200 words*)

Neutronic, thermal hydraulic, and thermal mechanical studies have been performed on an innovative vapor core nuclear reactor concept for space propulsion. The Nuclear Vapor Thermal Reactor (NVTR) Rocket Engine uses modified-NERVA geometry and systems with the solid fuel replaced by uranium tetrafluoride vapor. The use of C-C composite fuel elements in the NVTR leads to a compact reactor with low critical mass, good power peaking characteristics, an overall negative power coefficient of reactivity and, hence, good stability, and a propulsion system with high specific impulse. Thermo-mechanical analysis has shown excellent thermo-mechanical behavior under the high power density, high temperature NVTR environment. The NVTR is an intermediate term gas core thermal rocket engine with specific impulse in the range of 1000-1200 seconds; a thrust of 75,000 lbs. for a hydrogen flow rate of 30 kg/s; average core exit temperatures of 3100 K to 3400 K; reactor thermal powers of 1400 to 1800 MW; and thrust-to-weight ratios of 5-to-1.

14. SUBJECT TERMS

Nuclear thermal propulsion; Advanced reactor; Conceptual reactor design; Nuclear rocket

15. NUMBER OF PAGES

35

16. PRICE CODE

A03

17. SECURITY CLASSIFICATION OF REPORT	18. SECURITY CLASSIFICATION OF THIS PAGE	19. SECURITY CLASSIFICATION OF ABSTRACT	20. LIMITATION OF ABSTRACT
Unclassified	Unclassified	Unclassified	

National Aeronautics and
Space Administration

Lewis Research Center
21000 Brookpark Rd.
Cleveland, OH 44135-3191